ACS OMEGA

Open Access

http://pubs.acs.org/journal/acsodf

Article

Enhancing CO and H_2 Production in Propane Dry Reforming in Excess of CO_2

Emad Al-Shafei,* Mohammad Aljishi, Ahmed Alasseel, Anaam H. Al-ShaikhAli, and Mohammed Albahar

Cite This: *ACS Omega* 2024, 9, 17646−17654

Read Online

ACCESS | Metrics & More | Article Recommendations | Supporting Information

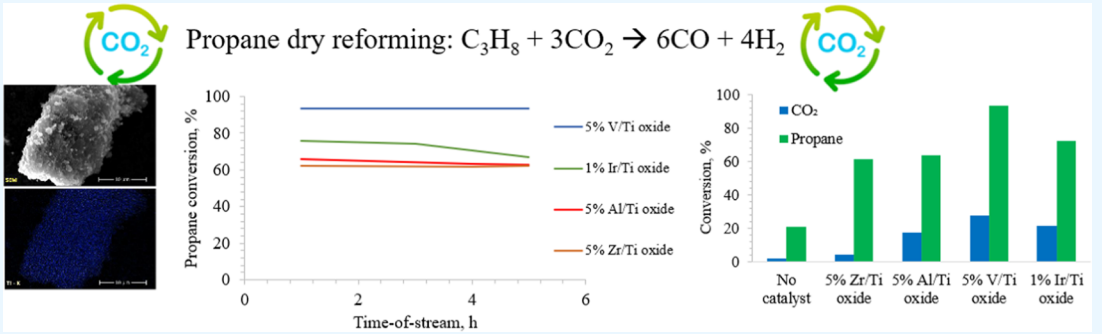

ABSTRACT: This study focuses on addressing the challenges in the dry reforming of propane, a process historically marked by low syngas yields and only moderate conversions of CO_2 and propane. The primary objective was to enhance CO_2 utilization and boost the selectivity of syngas (CO and H_2) production using titania-based catalysts. For synthesizing these catalysts, an impregnation method was employed with subsequent characterization through X-ray diffraction (XRD), N_2 adsorption−desorption, ammonia temperature-programmed desorption (TPD), and hydrogen temperature-programmed reduction (TPR). The titania-based catalysts generally possess weak acidic strength, with each catalyst displaying a unique reduction profile. The dry reforming process using these catalysts resulted in varying levels of propane conversion, with V/Ti, Ir/Ti, Al/Ti, and Zr/Ti catalysts showing distinct efficiencies. Notably, the Ir/Ti and V/Ti oxide catalysts achieved the lowest selectivity for generating intermediate byproducts such as methane, ethane, ethylene, and propylene while successfully promoting higher syngas CO and H_2 production alongside stable propane conversion. When exposed to excess CO_2, each catalyst consumed differing amounts of CO_2 molecules. Particularly, the Ir/Ti and V/Ti oxide catalysts demonstrated enhanced activity in promoting CO_2 reactions with intermediate radical species, facilitating carbon−carbon (C−C) bond dissociation and leading to increased syngas production. This study offers valuable insights into the potential of titania-based catalysts in improving the efficiency and selectivity of propane dry reforming processes for blue hydrogen.

1. INTRODUCTION

The growth in global sustainable energy demands more blue hydrogen for zero-emission vehicles and chemical plants.[1−3] Also, efforts to decarbonize the fossil fuel-based petrochemical industry have surged for more CO_2 capture and utilization. Dry reforming would be an attractive route to increase syngas production (CO and H_2).[4−6] Dry reforming of propane remains a challenging reaction, as it delivers low yields of syngas products with moderate conversion of both CO_2 and C2−C3[7−9] compared to the higher performance of methane dry reforming.[4,10] Figure 1 presents the thermodynamics of C1−C3 dry reforming in the form of Gibbs free energy versus temperature, showing that dry reforming of C2−C3 requires lower reaction temperatures than dry reforming of methane.[11,12] Specifically, propane appears more favorable at notably lower temperatures, while dry reforming of ethane and methane noticeably requires higher temperatures. Ultimately, the utilization of CO_2 for C2−C3 dry reforming produces more moles of CO and hydrogen, as described in eqs 1−3.

$$\text{dry reforming of methane: } CH_4 + CO_2 \rightarrow 2CO + 2H_2 (\Delta H^{\circ}_{298}\, 249\ \text{kJ mol}^{-1}) \quad (1)$$

$$\text{dry reforming of ethane: } C_2H_6 + 2CO_2 \rightarrow 4CO + 3H_2 (\Delta H^{\circ}_{298}\, 429.7\ \text{kJ mol}^{-1}) \quad (2)$$

Received: February 10, 2024
Revised: March 16, 2024
Accepted: March 20, 2024
Published: April 1, 2024

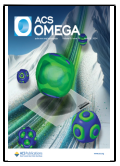

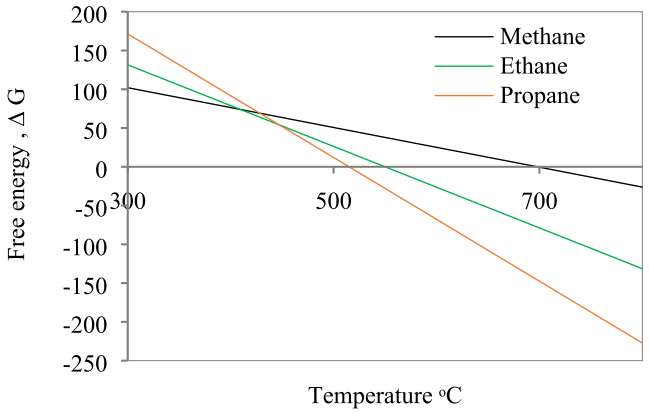

Figure 1. Thermodynamics of C1−C3 dry reforming.

$$\text{dry reforming of propane: } C_3H_8 + 3CO_2 \rightarrow 6CO + 4H_2 \left(\Delta H^{\circ}_{298}\ 621.3\ \text{kJ mol}^{-1}\right) \quad (3)$$

Several propane dry reforming studies utilized reactive catalysts based on Ni,[8] Ru,[13] Re,[14] and Rh,[7] supported by Al_2O_3,[13−15] ZrO_2,[7] TiO_2,[16] SiO_2,[16] CeO_2,[7,8] and MgO.[16] Solymosi et al.[16] studied the catalytic dry reforming of propane at 650 °C over various catalysts, highlighting that these catalysts with Al_2O_3 and TiO_2 supports loaded with Rh showed the low to moderate conversion of propane and CO_2 in the range of ∼40 to 70%. Moreover, catalyst supported by TiO_2 delivered the optimum CO/H_2 ratio in the range of 1.6−1.9.[16] Another study by Erdöhelyi et al.[17] investigated four catalyst supports for methane dry reforming (TiO_2, SiO_2, Al_2O_3, and MgO) and TiO_2, demonstrated as an effective support for the Rh catalyst in dry reforming, with no coke deposition made over the catalyst and the support. A similar observation was made by Bradford and Vannice;[18] they used NiO on various supports, among which was TiO_2, which provided better performance in the dry reforming of methane with no coke deposition.

As stated, the catalytic dry reforming of propane suffers from either low conversion or a low yield of syngas. The dry reforming of propane proceeds via carbon−carbon (C−C) bond dissociation; however, several byproducts, mainly methane and other gases, including ethane, ethylene, and propylene, are produced during dry reforming. The generation of such intermediate byproducts is attributed to the further complexity of the propane dry reforming reaction. Råberg et al.,[19] Jensen et al.,[20] and Solymosi et al.[14] discussed that the carbon−carbon bond dissociation of propane was the rate-limiting step over a NiO-based catalyst and found methane to be the main byproduct. Gomez et al.[8] studied the reaction at a low ratio of CO_2 to propane at 550 °C over bimetallic oxide catalysts based on CeO_2 with Ni, Co, and Pt, and they achieved low conversion of both propane and CO_2 (∼5 to 30%). Solymosi et al.[14] studied the effect of the CO_2/C3 ratio on the dry reforming of propane using a Re-based catalyst, and the result showed an increase in propane conversion from 50 to 80% as the CO_2 ratio increased.

Performing a dry reforming reaction of propane at high temperatures represents a promising approach to surpassing the thermodynamic conditions of the byproduct generated during dry reforming of propane. Siahvashi et al.[15] investigated dry reforming of propane at 700 °C and reported that the CO_2/C3 ratio of 3 was the optimum ratio over Ni- and Mo-based catalysts, while the specific selectivities toward CO and H_2 were not reported. Likewise, Sudhakaran et al.[21] studied the reaction over Fe- and Ni-based catalysts at 750 °C, and they achieved high conversion of CO_2 and propane (93 and 78%, respectively) but without reporting on the selectivity toward syngas production. Another study by Råberg et al.[19] utilized a Ni-based catalyst with cofeeding H_2 to increase the dry reforming of propane at 600 °C. They reported high conversions of CO_2 and propane (∼40 to 70 and ∼20 to 50%, respectively), while CO selectivity approached 95%. However, using cofeeding H_2 enabled the utilization of CO_2 for the generation of a higher CO product via the reverse water−gas shift (RWGS) reaction route. The yield of syngas of CO and H_2 obtained from dry reforming was affected by the conversion rate of propane and byproducts of methane.[14,22]

Erdöhelyi et al.[17] and Bradford and Vannice[18] investigated dry reforming of methane over supported catalysts of Rh and Ni oxides. They addressed the dissociation of methane into reactive intermediate radical species such as CH_3*, CH_2*, CH*, CH_xO*, HO*, and H*, which can react with adsorbed CO_2 to generate more CO, H_2, and H_2O products. Methane dry reforming is conducted at high temperatures but produces simple intermediates over the catalyst,[17] and the reaction is considered less complex compared to propane dry reforming.[14,22] In particular, Solymosi et al.[14,16] studied the propane dry reforming over Rh and Re catalysts using Fourier transform infrared (FTIR) and concluded that several intermediate surface species from propane were generated. Consequently, propane was not completely converted over the catalysts due to several byproducts and intermediates, including methane and ethane, which require higher reaction temperatures to proceed with full dry reforming. In this study, dry reforming was performed over a noble metal (1% Ir oxide), two transition metals (5% V oxide and 5% Zr oxide), and 5% Al oxide to increase acidic and basic properties supported over titania. Titania was demonstrated to be a promising support for methane dry reforming,[17] to investigate propane dry reforming performance in excess of CO_2 to overcome the byproducts obtained over the catalyst and targeting to increase syngas of CO and H_2 production and increase propane dry reforming conversion.

2. EXPERIMENTAL SECTION

2.1. Materials. Titanium(IV) oxide anatase phase, aluminum(III) nitrate, ammonium metavanadate, zirconium(IV) oxynitrate hydrate, and iridium(III) chloride purchased from Fisher Scientific and Alfa Aesar were utilized as precursors to synthesize titania-based catalysts.

2.2. Preparation of the Titania-Based Catalyst. The titania-based catalyst precursor was synthesized using the wet impregnation method[23,24] to prepare catalysts of 5% Zr (1.0 g), 5% Al (2.1 g), 5% V (0.32 g), and 1% Ir (0.062 g) over the Ti oxide support. The dissolved catalyst salt in RO water was mixed with diluted nitric acid (0.10 N, 50 mL) at 40−50 °C and stirred for 60 min. 5 g of TiO_2 powder was added to the dissolved metal salt in the solution and stirred for 6 h. The precursor of the catalyst was separated from the aqueous solution using a centrifuge, and the catalyst powder was transferred to a vacuum drying oven for 24 h at 85 °C. Finally, the titania-based catalyst precursor was calcined at 700 °C for 5 h.

2.3. Characterization. The crystalline phases of calcined titania-based catalysts were identified by X-ray diffraction (XRD) using a PANalytical X'Pert PRO Diffractometer. The

https://doi.org/10.1021/acsomega.4c01338
ACS Omega 2024, 9, 17646−17654

morphologies of the catalyst surfaces and elemental mapping were determined by using scanning electron microscopy (SEM) and energy dispersive X-ray spectroscopy (EDS), respectively, using an FEI Quanta 400 instrument. The textural properties of the catalysts were analyzed by N_2 adsorption−desorption using a Micromeritics ASAP 2420 instrument. Furthermore, the catalyst surface acidity was measured by ammonia temperature-programmed desorption (NH_3-TPD)[25] using a HIDEN CATLAB instrument. Moreover, catalyst reduction experiments were carried out by the hydrogen temperature-programmed reduction (H_2-TPR) technique using a Micromeritics Autochem 2910 instrument.

2.4. Catalyst Activity Test. The dry reforming of propane was conducted using a quartz fixed-bed reactor, which was placed into a vertical high-temperature furnace. 0.45 g of the titania-based catalyst was preheated at 600 °C at atmospheric pressure with a nitrogen flow rate of 50 mL min^{-1} for 2 h. The mole ratio of the CO_2 and propane gas mixture was adjusted at 20:1 with 3 mL min^{-1} flow via mass flow controllers to the catalytic reactor. The gas produced from the reactor was determined using online gas chromatography equipped with a thermal conductivity detector from Agilent. The dry reforming conversion, selectivity, and yield of H_2 and CO are calculated as described in eqs 4 and 5.[23,26]

$$\text{conversion of } CO_2 \text{ or propane (mol\%)} = \frac{\text{feed in} - \text{feed out}}{\text{feed in}} \times 100 \quad (4)$$

$$\text{hydrogen or product selectivity (mol\%)} = \frac{H_2 \text{ mol produced}}{\text{prodcut mol}} \times 100 \quad (5)$$

3. RESULTS AND DISCUSSION

3.1. Catalyst Crystalline Determination and Textural Properties. The XRD analysis showed the patterns of impregnated titania-based catalysts, as shown in Figure 2.

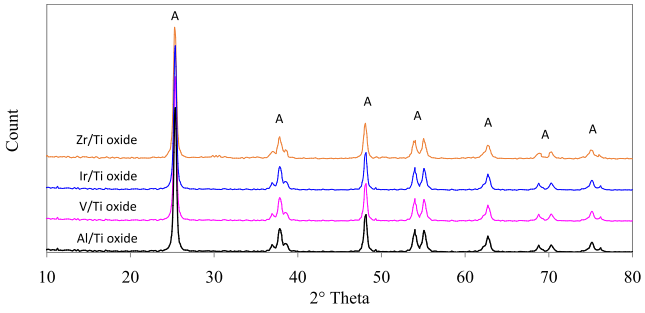

Figure 2. XRD chromatogram of titania-based catalysts (A: anatase of TiO_2).

The XRD patterns of the four catalysts showed only the anatase crystalline form without the appearance of any rutile phase of titania; however, there is no appearance of any crystal from the impregnated metal oxide catalyst. This is attributed to the low concentration of metal oxide loading, which is aligned with observations noted in early studies.[27,28] The textural properties of titania-based catalysts were evaluated, and it was observed that the catalysts exhibited low surface areas (27−94 m^2/g), with pore volumes between 0.19 and 0.23 cm^3/g, as presented in Table 1. Zr, Al, Ir, and V oxides supported by titania were identified in the EDS mapping, and the SEM micrographs confirmed the uniform dispersion of metal oxide over the TiO_2 support (Figure 3A−D). The metal composition over the support was determined (Table S1), revealing a slight alteration in the concentration of impregnated metals within the prepared catalyst during its synthesis.

3.2. Reducibility of the Catalysts. Figure 4A shows the H_2-TPR diagrams of the four titania-based catalysts and a TiO_2 support as a reference. Each catalyst showed different reduction peaks over TiO_2, which indicated that each catalyst was impregnated over the support, despite the dopant being undetectable by XRD analysis. The reduction graph of the TiO_2 support used as a reference consists of two reduced peaks. The maximum temperature peak (T_{max}) was detected at high-temperature reduction between 650 and 820 °C attributed to the reduction of Ti^{4+} oxide to Ti^{3+} oxide with further reduction at >820 °C to Ti^{3+} oxide.[29] Similarly, Al/Ti and Zr/Ti oxide catalysts showed no reduction peaks of ZrO_2 and Al_2O_3 over the TiO_2 support below <550 °C due to the poor reducibility of both metal oxides,[30] while the reeducation peak at >550 °C is attributed to the reduction of Al−O−Ti and Zr−O−Ti along with reduction of Ti^{4+} oxide to Ti^{3+} oxide. On the other hand, the middle-range reduction peaks showed by V/Ti and Ir/Ti are attributed to the reduction of the metal oxide dopant over TiO_2 between 200 and 650 °C, as observed in earlier studies,[31−33] which is essential to promote reaction activity.

3.3. Catalyst Acidity. The catalyst acidity of the prepared titania-based catalysts was analyzed by NH_3-TPD. Figure 4B shows that each titania-based catalyst has slightly different acidity strength compared to the others. While the Zr/Ti oxide catalyst showed a wider acidity peak from 150 to 650 °C among other catalysts, the observed acidity peak of NH_3 desorption for the Al/Ti oxide catalyst shifted between 100 and 550 °C.[34,35] Table 1 lists the surface acidity of each catalyst, and it was observed that they had low acidity in the following order TiO_2 < Ir/Ti < V/Ti < Zr/Ti < Al/Ti.

3.4. Catalyst Basicity. Ultimately, the surface basicity of titania-based catalysts was enhanced, with the CO_2 adsorption being much more prominent compared to the original basic sites of TiO_2, as shown in Figure 5. Ye et al.[36] observed that titania-based catalysts showed strong chemisorption of CO_2, which was retained considerably at higher temperatures between 600 and 1200 °C. The CO_2 adsorption over titania-based catalysts is illustrated in Table 1, and three CO_2 desorption temperature regions of basic sites were recognized over titania-based catalysts.[37−39] The first region is the weak basic sites of CO_2 between temperatures 35 and 325 °C, likely related to bicarbonate species,[38−42] while the stronger basic sites at higher-temperature CO_2-TPD at 325−725 °C represented the bidentate carbonate intermediate with strong sites of CO_2 linked with the less oxide coordination state of titania-based catalysts and were likely related to basic surface oxygen anions.[38,39,43−46] The highest temperature region >725 °C represented the oxycarbonate, which is attributed to strong basic sites and favors high-temperature decomposition.[38,39] Specifically, the addition of noble and transition metals to titania-based catalysts led to significantly more basic sites, indicated by the more than 1.7−2.7-fold increase in peak intensity between 35 and 725 °C incorporated with TiO_2, compared to the original support. The amounts of basic sites decreased in the following order TiO_2 < Zr/Ti < Ir/Ti < Al/Ti

https://doi.org/10.1021/acsomega.4c01338
ACS Omega 2024, 9, 17646−17654

Table 1. BET, NH_3-TPD, and CO_2-TPD of Titania-Based Catalysts[a]

catalyst	BET surface area, m^2/g	pore volume cm^3/g	average pore diameter, nm	adsorbed NH_3 μmol/g	adsorbed CO_2 35−325 °C[i] mmol/g	adsorbed CO_2 325−725 °C[ii] mmol/g	adsorbed CO_2 >725 °C[iii] mmol/g
Ti oxide	11	0.10	38.1	45			
5% Zr/Ti oxide	27	0.22	34	215	0.74	2.55	2.19
5% Al/Ti oxide	94	0.19	85	220	1.41	4.89	12.85
5% V/Ti oxide	55	0.20	125	205	1.33	5.87	11.22
1% Ir/Ti oxide	45	0.24	140	190	1.14	3.48	9.57

[a](i) Weak basic sites and (ii) strong basic sites of the bidentate carbonate intermediate and (iii) strong basic sites of oxycarbonate.

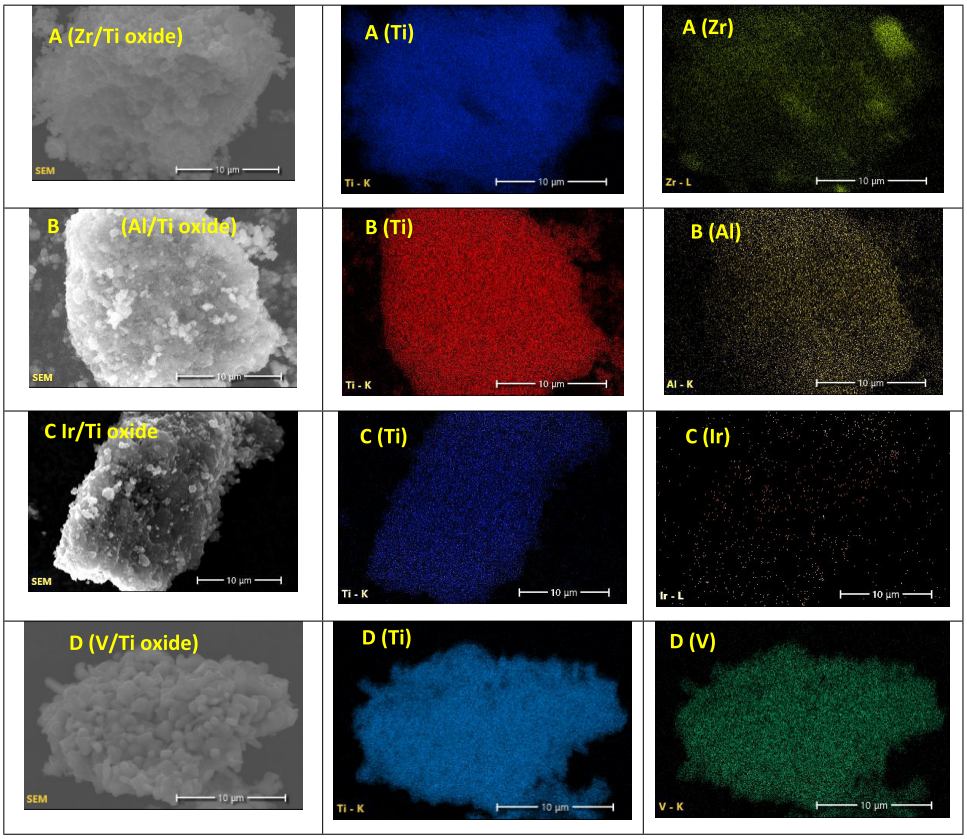

Figure 3. SEM and EDS metal mapping of titania-based catalysts: (A) Zr/Ti oxide, (B) Al/Ti oxide, (C) Ir/Ti oxide, and (D) V/Ti oxide.

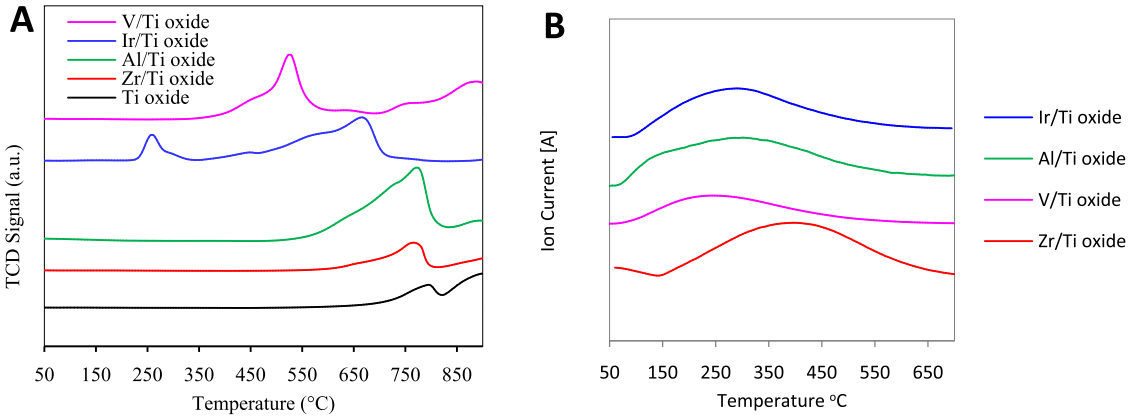

Figure 4. (A) H_2-TPR and (B) NH_3-TPD diagrams of titania-based catalysts.

https://doi.org/10.1021/acsomega.4c01338
ACS Omega 2024, 9, 17646−17654

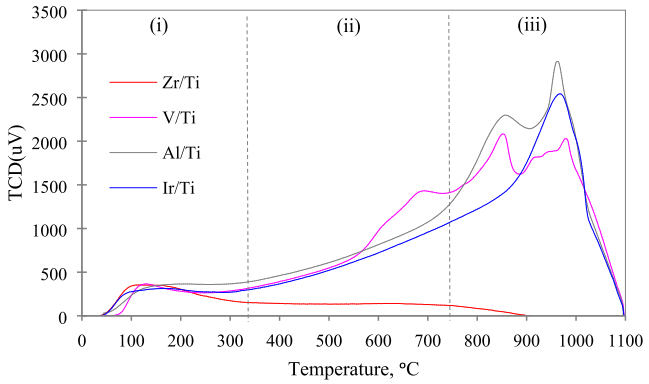

Figure 5. CO_2-TPD diagram of titania-based catalysts [(i) weak basic sites and (ii) strong basic sites of the bidentate carbonate intermediate and (iii) strong basic sites of oxycarbonate].

< V/Ti, as shown in Table 1. Overall, the titania-based catalysts exhibited little increase in acidity and a significant increase in basic sites, which are essential conditions for surface adsorption to accommodate more CO_2 for the bidentate carbonate intermediate[47] and C−C bond dissociation[48] reactions, which are the main desired reactions for higher dry reforming of propane.

3.5. CO_2 and Propane Conversion over Titania-Based Catalysts. The study investigated the use of excess CO_2 to maximize its utilization and limit the production of multiple dry reforming byproducts (methane, ethane, ethylene, and propylene) that may reduce syngas (CO and H_2) production. The titania-based catalysts were demonstrated to be highly reactive catalysts for the dry reforming reaction due to an increase in the surface acidity and basicity (Figures 4B and 5), achieving high propane conversions that increased from 21% without a catalyst to 93 and 72.4% over V/Ti and Ir/Ti oxide catalysts, respectively. Similar ranges of propane dry reforming conversions were obtained by Sudhakaran et al.[21] while the reforming was conducted at a higher temperature (750 °C) over a NiCe oxide-based catalyst. Each catalyst showed different conversions of CO_2, as shown in Figure 6. Ultimately,

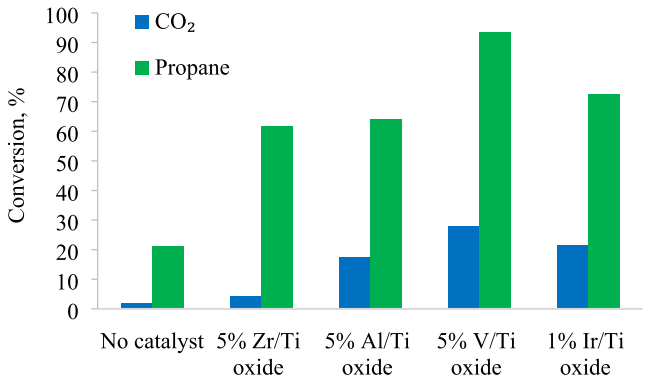

Figure 6. Dry reforming of propane at 600 °C in excess of CO_2: propane and CO_2 conversion.

both CO_2 and propane conversion increased for each catalyst in the following order of Zr/Ti < Al/Ti < Ir/Ti < V/Ti oxide catalysts. The catalytic stability test of propane conversion during dry reforming was investigated using four catalysts at 600 °C. Figure 7 shows the time-on-stream (TOS) of propane dry reforming performance for 5 h and a successfully stable

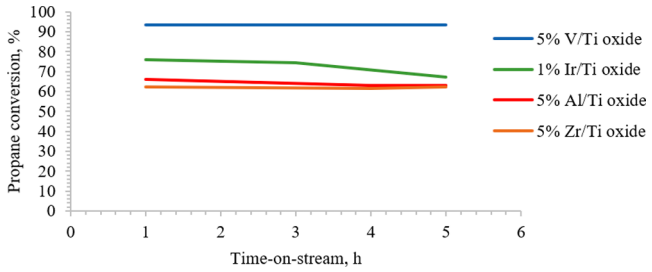

Figure 7. Time-on-stream of propane conversion at 600 °C in excess of CO_2.

conversion of propane over four catalysts. The V/Ti oxide catalyst showed the highest conversion of propane, followed by Ir/Ti oxide. The carbon balance of propane dry reforming over Ir, V, Al, and Zr over TiO_2 catalysts is shown in Table S6 with a deviation of ±5%.

The actual molar consumption ratio of CO_2 per propane (mol/mol) during the dry reforming reaction was analyzed, as presented in Figure 8. It was calculated that the CO_2/propane

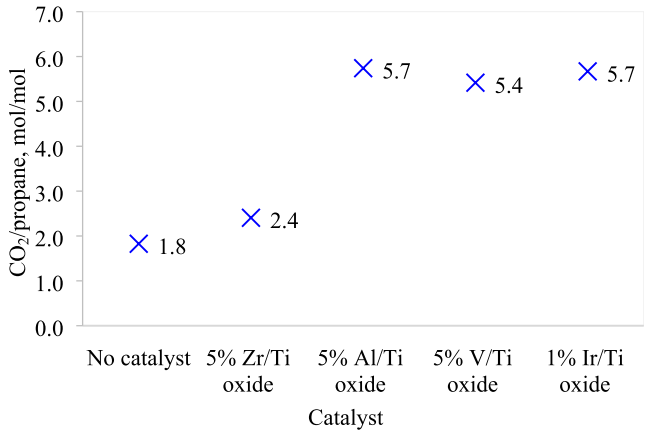

Figure 8. Consumed CO_2 during propane dry reforming at 600 °C in excess of CO_2.

ratio consumed during propane dry reforming was in the range of 5.4−5.7 for the Al/Ti and Ir/Ti catalysts. On the other hand, the V/Ti oxide catalyst utilized the highest CO_2/propane ratio, consuming around 5.7 CO_2 moles per mole of propane. In contrast, a low CO_2/propane ratio was maintained over the Zr/Ti oxide catalyst (around 2.4), which is slightly higher than noncatalytic dry reforming, which was around 1.8. Accordingly, the catalytic dry reforming of propane over titania-based catalysts based on titania support showed higher CO_2 consumption levels than the theoretically suggested CO_2/propane ratio in the range of 3.[15,21] The presence of excess CO_2 derived more bidentate carbonate intermediate, which enabled each catalyst to additionally consume different amounts of CO_2, depending on the extent of reaction routes between CO_2 and intermediate radical species generated during carbon−carbon bond dissociation of propane over each catalyst.

3.6. Product Selectivity over Titania-Based Catalysts. The selectivity of syngas and byproducts from propane dry reforming was investigated over all prepared titania-based catalysts supported by titania. Although high propane and CO_2 conversions were achieved in excess of CO_2, as depicted in Figure 6, the generation of byproducts limited the extent of the

https://doi.org/10.1021/acsomega.4c01338
ACS Omega 2024, 9, 17646−17654

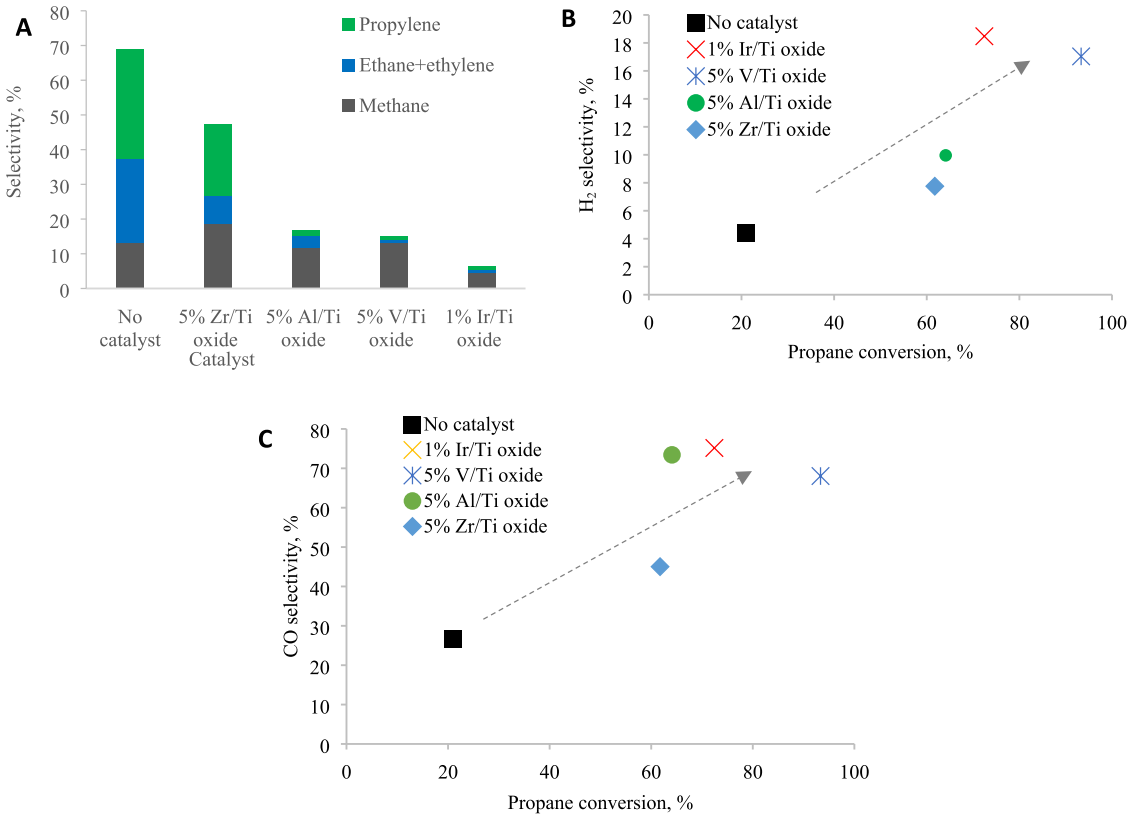

Figure 9. (A) Selectivity of byproducts versus H_2. (B) Selectivity of H_2 versus propane conversion. (C) Selectivity of CO versus CO_2 conversion of dry reforming over titania-based catalysts in excess of CO_2 at 600 °C.

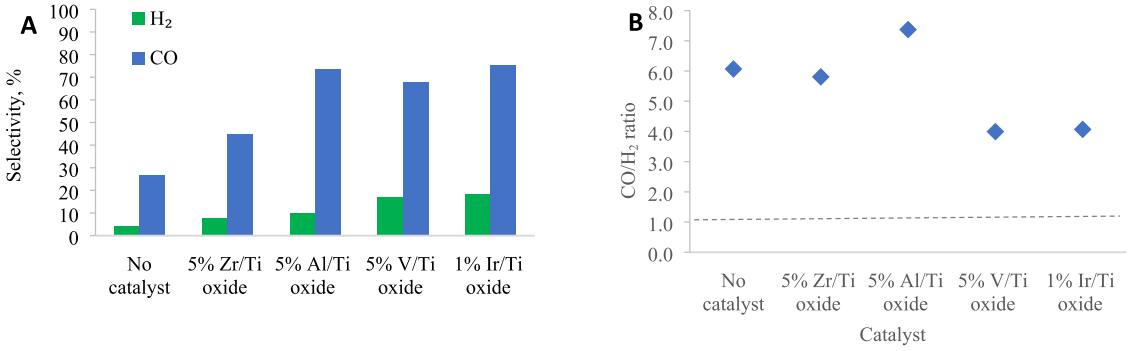

Figure 10. (A) Selectivity of H_2 versus CO. (B) CO/H_2 ratio of dry reforming of propane using titania-based catalysts in excess of CO_2 at 600 °C.

increase in dry reforming performance. Figure 9A shows that the highest byproduct (methane, ethane, ethylene, propylene) selectivity (47.2%) was obtained from a dry reforming reaction of the 5% Zr/Ti oxide catalyst. In contrast, the selectivity of byproducts dropped significantly to 6.4% when the Ir/Ti catalyst was introduced for dry propane reforming. Methane gas was the main observed byproduct from propane dry reforming, indicative of more carbon−carbon bond dissociation of propane over the catalyst, as observed by Raberg et al.[19] In comparison, the Ir/Ti catalyst delivered a higher hydrogen selectivity (18.5%) than V/Ti (17%, Figure 9B). Similarly, the V/Ti oxide catalyst showed the highest propane conversion of around 93% (Figure 6) and showed a low byproduct selectivity of methane, ethane, ethylene, and propylene of around 14.9%. Moreover, the highest selectivity to byproducts during catalytic dry reforming was obtained over Al/Ti and Zr/Ti and was around 16.6 and 47.2%, respectively. Figure 9B,C shows the increase in hydrogen and carbon monoxide selectivities with the increase in propane conversion. Specifically, the Ir/Ti, Al/Ti, and V/Ti oxide catalysts achieved the highest selectivity toward hydrogen and carbon monoxide. The lower hydrogen selectivities obtained for some catalysts are attributed to the reaction of CO_2 with intermediate radical species (e.g., methyl radicals) and reverse water−gas shift (RWGS), which tend to produce more CO rather than hydrogen abstraction via the dehydrogenation route, as described in eqs 6 and 7.

$$\text{reaction of intermediate with adsorbed } CO_2\text{: } CH_3{}^* + CO_2{}^* \rightarrow CH_3O^* + CO + {}^* \quad (6)$$

$$H^* \text{ react with } CO_2{}^* \text{ via RWGS reaction: } CO_2{}^* + H^* \rightarrow CO + HO^* + {}^* \quad (7)$$

https://doi.org/10.1021/acsomega.4c01338
ACS Omega 2024, 9, 17646−17654

3.7. Syngas versus the CO/H_2 ratio. Figure 10A,B shows syngas (CO and H_2) selectivity and the CO/H_2 ratio obtained from propane dry reforming over synthesized four titania-based catalysts. In excess of CO_2, the thermal noncatalytic dry reforming route showed a substantial level of CO selectivity (26.8%), indicating that H_2 was considerably consumed through the RWGS reaction. Utilizing the Zr/Ti oxide catalyst increased the CO selectivity to be 5.8 times higher than that for H_2. Although the highest CO selectivity was achieved over the Al/Ti (73.4%), V/Ti (68%), and Ir/Ti (75.2%) oxide catalysts, the CO/H_2 ratio decreased from 7.4 to ∼4, higher than the theoretical value (2.5; eq 3). The adsorbed CO_2 promoted the reactions with intermediate radical species from propane bond dissociation of C−C and promoted more RWGS reactions, leading to the production of more CO product. The CO/H_2 ratio gradually declined over V/Ti and Ir/Ti oxide catalysts as a result of more hydrogen being released from the catalyst surface from the C−H bond dissociation,[16] as described by eqs 8 and 9.

$$\text{dehydrogenation of propane: } C_3H_8{}^* + 2^* \rightarrow C_3H_6{}^* + 2H^* \quad (8)$$

$$\text{C} - \text{C bond dissociation: } 2C_3H_8{}^* + 4^* \rightarrow C_2H_4{}^* + C_2H_5{}^* + CH_3{}^* + CH_2{}^* + 2H^* \quad (9)$$

$$\text{dehydrogenation of propane: } C_3H_8{}^* + 2^* \rightarrow C_3H_6{}^* + 2H^* \quad (10)$$

$$\text{byproduct of methane: } CH_3{}^* + H^* \rightarrow CH_4{}^* + {}^* \quad (11)$$

$$\text{byproduct of ethane: } C_2H_5{}^* + H^* \rightarrow C_2H_6{}^* + {}^* \quad (12)$$

$$\text{byproduct of ethylene: } C_2H_4{}^* \rightarrow C_2H_4 + {}^* \quad (13)$$

Accordingly, excess of the CO_2/propane ratio by introducing more CO_2 to the reaction was shown to be an effective approach in improving conversions in propane dry reforming at 600 °C.[14] Specifically, adsorption of more CO_2 over the catalyst permitted more reactions with radical intermediate species, thereby limiting the byproduct of propylene, ethylene ethane, and methane over the Ir/Ti, V/Ti, and Al/Ti oxide catalysts. The C−C bond dissociation of propane over the catalyst results in forming several radical intermediate species that can react with adsorbed hydrogen to generate undesired byproducts such as ethane and methane via the hydrogenation route, as described in eqs 9−13. Erdöhelyi et al.[17] demonstrated that the reaction of adsorbed CO_2 with the radical intermediate species of methane (CH_3*, CH_2*, CH*, and H*) led to more CO, H_2, and intermediate hydroxide (HO*). Bradford and Vannice[18] noted that adsorbed hydroxide is a reactive radical that can participate in reactions with intermediate radical species to generate more H* and H_2O. Likewise, in a large amount of CO_2, intermediate species based on ethylene and ethane (C_2H_x*) would also be readily reactive with adsorbed CO_2, causing more CO formation.

In summary, the synthesized titania-based catalysts displayed a unique combination of surface acidity and basicity, which was instrumental in achieving a high level of CO_2 utilization. This was evidenced by CO_2/propane consumption ratios ranging between 5.4 and 5.7, particularly noted in the Al/Ti, Ir/Ti, and V/Ti oxide catalysts. Among these, the Ir/Ti and V/Ti oxide catalysts stood out for their higher middle-range reduction peaks, indicating their enhanced reactivity and efficiency in converting propane.

The V/Ti oxide catalyst was particularly noteworthy for its 14.9% selectivity toward byproducts, primarily consisting of methane, ethane, ethylene, and propylene. On the other hand, the Ir/Ti catalyst demonstrated the lowest selectivity toward such byproducts, including methane, highlighting its superior selectivity for hydrogen production. This suggests that while both catalysts are highly effective in propane conversion, they exhibit distinct selectivity profiles, with the Ir/Ti catalyst showing a marked propensity for hydrogen generation. These findings underscore the potential of these titania-based catalysts in refining the processes of propane conversion and syngas production. Future studies will extend time-on-stream experiments to more thoroughly evaluate catalyst stability, conversion, and syngas selectivity, especially for the Ir/Ti catalyst.

4. CONCLUSIONS

In the study of propane dry reforming with excess of CO_2, Ir/Ti and V/Ti oxide catalysts emerged as highly reactive options. These titania-based catalysts displayed an increase in surface acidity and a notable augmentation in basic sites, particularly in bidentate carbonate intermediates. This enhancement is essential, as it creates an optimal surface condition for adsorption, allowing for increased accommodation of CO_2 and propane. This, in turn, facilitates more effective C−C bond dissociation, which is key to achieving a higher efficiency in dry reforming. Remarkably, the highest propane conversion was achieved with these catalysts, specifically Ir/Ti and V/Ti, due to their superior ability to dissociate C−C bonds and their high selectivity for hydrogen abstraction via the C−H dehydrogenation of propane. Furthermore, both catalysts made the highest CO selectivity, attributed to the promotion of more CO_2 reactions with intermediate radical species arising from C−C bond dissociation in propane, as well as from the reverse water−gas shift (RWGS) reaction. The study also highlighted that the presence of excess CO_2 allowed each catalyst to consume varying amounts of CO_2. This consumption is dependent on the extent of the reaction pathways between CO_2 and the intermediate radical species, indicating a stable interaction between the catalysts and the reactive environment. This conclusion underscores the potential of Ir/Ti and V/Ti oxide catalysts in enhancing the efficiency and selectivity of propane dry reforming processes, particularly under CO_2-rich conditions.

■ ASSOCIATED CONTENT

Supporting Information

The Supporting Information is available free of charge at https://pubs.acs.org/doi/10.1021/acsomega.4c01338.

Composition of catalyst samples used in propane dry reforming by SEM-EDS analysis (Table S1); EDS metal content of the V/Ti oxide catalyst (Table S2); EDS metal content of the Al/Ti oxide catalyst (Table S3); EDS metal content of the Ir/Ti oxide catalyst (Table S4); EDS metal content of the Zr/Ti oxide catalyst (Table S5); carbon balance (mol %) of propane dry reforming over catalysts: time-on-stream of propane conversion at 600 °C in excess of CO_2 (Table S6); and

https://doi.org/10.1021/acsomega.4c01338
ACS Omega 2024, 9, 17646−17654

time-on-stream of propane conversion at 600 °C in excess of CO_2 (PDF)

AUTHOR INFORMATION

Corresponding Author

Emad Al-Shafei − *Research and Development Center, Saudi Aramco, Dhahran 31311, Saudi Arabia;* orcid.org/0000-0003-3832-1056; Email: shafeien@aramco.com, emadnaji@gmail.com

Authors

Mohammad Aljishi − *Research and Development Center, Saudi Aramco, Dhahran 31311, Saudi Arabia*

Ahmed Alasseel − *Research and Development Center, Saudi Aramco, Dhahran 31311, Saudi Arabia*

Anaam H. Al-ShaikhAli − *Research and Development Center, Saudi Aramco, Dhahran 31311, Saudi Arabia*

Mohammed Albahar − *Research and Development Center, Saudi Aramco, Dhahran 31311, Saudi Arabia;* orcid.org/0000-0002-8009-5980

Complete contact information is available at: https://pubs.acs.org/10.1021/acsomega.4c01338

Notes

The authors declare no competing financial interest.

ACKNOWLEDGMENTS

The authors would like to acknowledge the support provided by R&DC Saudi Aramco.

REFERENCES

(1) Kannah, R. Y.; Kavitha, S.; Karthikeyan, O. P.; Kumar, G.; Dai-Viet, N. V.; Banu, J. R. Techno-economic assessment of various hydrogen production methods–A review. *Bioresour. Technol.* **2021**, *319*, No. 124175, DOI: 10.1016/j.biortech.2020.124175.

(2) Kumar, G.; Eswari, A. P.; Kavitha, S.; Kumar, M. D.; Kannah, R. Y.; How, L. C.; Muthukaruppan, G.; Banu, J. R. Thermochemical conversion routes of hydrogen production from organic biomass: processes, challenges and limitations. *Biomass Convers. Biorefin.* **2020**, *13*, 8509−8534, DOI: 10.1007/s13399-020-01127-9.

(3) Sharma, M.; Schoegl, I. A comparative assessment of homogeneous propane reforming at intermediate temperatures. *Int. J. Hydrogen Energy* **2013**, *38* (30), 13272−13281.

(4) Shah, Y. T.; Gardner, T. H. Dry reforming of hydrocarbon feedstocks. *Catal. Rev.* **2014**, *56* (4), 476−536.

(5) Alipour, Z.; Borugadda, V.B.; Wang, H.; Dalai, A. K. Syngas production through dry reforming: A review on catalysts and their materials, preparation methods and reactor type. *Chem. Eng. J.* **2023**, *452*, No. 139416, DOI: 10.1016/j.cej.2022.139416.

(6) Luo, Y.; Chen, J.; and; Wang, T. Evaluation of the Effect of CaO on Hydrogen Production by Sorption-Enhanced Steam Methane Reforming. *ACS Omega* **2024**, *9*, 5330−5337, DOI: 10.1021/acsomega.3c05918.

(7) Alabdullah, M.; Ibrahim, M.; Dhawale, D.; Bau, J. A.; Harale, A.; Katikaneni, S.; Gascon, J. Rhodium Nanoparticle Size Effects on the CO2 Reforming of Methane and Propane. *ChemCatChem.* **2021**, *13*, 2879−2886, DOI: 10.1002/cctc.202100063.

(8) Gomez, E.; Xie, Z.; Chen, J. G. The effects of bimetallic interactions for CO2-assisted oxidative dehydrogenation and dry reforming of propane. *AIChE J.* **2019**, *65* (8), No. e16670.

(9) Ronda-Lloret, M.; Marakatti, V. S.; Sloof, W. G.; Delgado, J. J.; Sepúlveda-Escribano, A.; Ramos-Fernandez, E. V.; Rothenberg, G.; Shiju, N. R. Butane Dry Reforming Catalyzed by Cobalt Oxide Supported on Ti2AlC MAX Phase. *ChemSusChem* **2020**, *13* (23), 6401.

(10) Świrk, K.; Rønning, M.; Motak, M.; Beaunier, P.; Da Costa, P.; Grzybek, T. Ce-and Y-modified double-layered hydroxides as catalysts for dry reforming of methane: on the effect of Yttrium promotion. *Catalysts* **2019**, *9* (1), 56.

(11) Gao, J.; Hou, Z.; Lou, H.; Zheng, X. Dry (CO2) reforming In *Fuel Cells: Technologies for Fuel Processing*; Elsevier, 2011; pp 191−221.

(12) Savchenko, V. I.; Zimin, Y. S.; Nikitin, A. V.; Sedov, I. V.; Arutyunov, V. S. Utilization of CO2 in non-catalytic dry reforming of C1–C4 hydrocarbons. *J. CO2 Util.* **2021**, *47*, No. 101490.

(13) Sutton, D.; Moisan, J.-F.; Ross, J. R. H. Kinetic study of CO2 reforming of propane over Ru/Al2O3. *Catal. Lett.* **2001**, *75* (3−4), 175−181.

(14) Solymosi, F.; Tolmacsov, P.; Zakar, T. S. Dry reforming of propane over supported Re catalyst. *J. Catal.* **2005**, *233* (1), 51−59.

(15) Siahvashi, A.; Chesterfield, D.; Adesina, A. A. Propane CO2 (dry) reforming over bimetallic Mo–Ni/Al2O3 catalyst. *Chem. Eng. Sci.* **2013**, *93*, 313−325.

(16) Solymosi, F.; Tolmacsov, P.; Kedves, K. CO2 reforming of propane over supported Rh. *J. Catal.* **2003**, *216* (1−2), 377−385.

(17) Erdöhelyi, A.; Cserényi, J.; Solymosi, F. Activation of CH4 and its reaction with CO2 over supported Rh catalysts. *J. Catal.* **1993**, *141* (1), 287−299.

(18) Bradford, M. C. J.; Vannice, M. A. Catalytic reforming of methane with carbon dioxide over nickel catalysts II. Reaction kinetics. *Appl. Catal., A* **1996**, *142* (1), 97−122.

(19) Råberg, L. B.; Jensen, M. B.; Olsbye, U.; Daniel, C.; Haag, S.; Mirodatos, C.; Sjåstad, A. O. Propane dry reforming to synthesis gas over Ni-based catalysts: influence of support and operating parameters on catalyst activity and stability. *J. Catal.* **2007**, *249* (2), 250−260, DOI: 10.1016/j.jcat.2007.04.004.

(20) Jensen, M. B.; Råberg, L. B.; Sjåstad, A. O.; Olsbye, U. Mechanistic study of the dry reforming of propane to synthesis gas over a Ni/Mg (Al) O catalyst. *Catal. Today* **2009**, *145* (1−2), 114−120.

(21) Sudhakaran, M. S. P.; Sultana, L.; Hossain, M. M.; Pawlat, J.; Diatczyk, J.; Brüser, V.; Reuter, S.; Mok, Y. S. Iron–ceria spinel (FeCe2O4) catalyst for dry reforming of propane to inhibit carbon formation. *J. Ind. Eng. Chem.* **2018**, *61*, 142−151, DOI: 10.1016/j.jiec.2017.12.011.

(22) García-Diéguez, M.; Herrera, C.; Larrubia, M. Á.; Alemany, L. J. CO2-reforming of natural gas components over a highly stable and selective NiMg/Al2O3 nanocatalyst. *Catal. Today* **2012**, *197* (1), 50−57.

(23) Al-Shafei, E. N.; Brown, D. R.; Katikaneni, S. P.; Al-Badairy, H.; Muraza, O. CO2-assisted propane dehydrogenation over of zirconia-titania catalysts: Effect of the carbon dioxide to propane ratios on olefin yields. *J. Environ. Chem. Eng.* **2021**, *9* (1), No. 104989.

(24) Takahashi, N.; Suda, A.; Hachisuka, I.; Sugiura, M.; Sobukawa, H.; Shinjoh, H. Sulfur durability of NOx storage and reduction catalyst with supports of TiO2, ZrO2 and ZrO2-TiO2 mixed oxides. *Appl. Catal., B* **2007**, *72* (1−2), 187−195.

(25) Abahussain, A. A. M.; Al-Fatesh, A. S.; Rajput, Y. B.; Osman, A. I.; Alreshaidan, S. B.; Ahmed, H.; Fakeeha, A. H.; Al-Awadi, A. S.; El-Salamony, R. A.; Kumar, R. Impact of Sr Addition on Zirconia−Alumina-Supported Ni Catalyst for CO x-Free CH4 Production via CO2Methanation. *ACS Omega* **2024**, *9*, 9309−9320, DOI: 10.1021/acsomega.3c08536.

(26) Sudhakaran, M. S. P.; Hossain, M.; Gnanasekaran, G.; Mok, Y. S. Dry reforming of propane over γ-Al2O3 and nickel foam supported novel SrNiO3 perovskite catalyst. *Catalysts* **2019**, *9* (1), 68 DOI: 10.3390/catal9010068.

(27) Vishwanathan, V.; Roh, H.-S.; Kim, J.-W.; Jun, K.-W. Surface properties and catalytic activity of TiO 2–ZrO 2 mixed oxides in dehydration of methanol to dimethyl ether. *Catal. Lett.* **2004**, *96* (1−2), 23−28, DOI: 10.1023/B:CATL.0000029524.94392.9f.

(28) Neppolian, B.; Wang, Q.; Yamashita, H.; Choi, H. Synthesis and characterization of ZrO2–TiO2 binary oxide semiconductor

nanoparticles: application and interparticle electron transfer process. *Appl. Catal., A* **2006**, *96* (1), 23−28.
(29) Liu, H.; Su, Y.; Hu, H.; Cao, W.; Chen, Z. An ionic liquid route to prepare mesoporous ZrO2−TiO2 nanocomposites and study on their photocatalytic activities. *Adv. Powder Technol.* **2013**, *24* (3), 683−688.
(30) Al-Shafei, E. N.; Albahar, M. Z.; Aljishi, M. F.; Aljishi, A. N. CO2 coupling reaction with methane by using trimetallic catalysts. *J. Environ. Chem. Eng.* **2021**, *9* (5), No. 106152.
(31) State, R.; Scurtu, M.; Miyazaki, A.; Papa, F.; Atkinson, I.; Munteanu, C.; Balint, I. Influence of metal-support interaction on nitrate hydrogenation over Rh and Rh-Cu nanoparticles dispersed on Al2O3 and TiO2 supports. *Arabian J. Chem.* **2017**, *10* (7), 975−984.
(32) Lian, Z.; Liu, F.; He, H. Effect of preparation methods on the activity of VO x/CeO 2 catalysts for the selective catalytic reduction of NO x with NH 3. *Catal. Sci. Technol.* **2015**, *5* (1), 389−396.
(33) Hernández-Cristóbal, O.; Diaz, G.; Gómez-Cortés, A. Effect of the reduction temperature on the activity and selectivity of titania-supported iridium nanoparticles for methylcyclopentane reaction. *Ind. Eng. Chem. Res.* **2014**, *53* (24), 10097−10104.
(34) Zhang, S.; Guo, Y.; Li, X.; Wu, X.; Li, Z. The double peaks and symmetric path phenomena in the catalytic activity of Pd/Al2O3-TiO2 catalysts with different TiO2 contents. *J. Solid State Chem.* **2018**, *262*, 335−342.
(35) Camposeco, R.; Castillo, S.; Mejía-Centeno, I.; Navarrete, J.; Nava, N. Boosted surface acidity in TiO2 and Al2O3-TiO2 nanotubes as catalytic supports. *Appl. Surf. Sci.* **2015**, *356*, 115−123.
(36) Ye, L.; Zhang, M.; Huang, P.; Guo, G.; Hong, M.; Li, C.; Irvine, J. T.; Xie, K. Enhancing CO2 electrolysis through synergistic control of non-stoichiometry and doping to tune cathode surface structures. *Nat. Commun.* **2017**, *8* (1), No. 14785, DOI: 10.1038/ncomms14785.
(37) Ahadzadeh, M.; Alavi, S. M.; Rezaei, M.; Akbari, E. Propane dry reforming over highly active NiO-MgO solid solution catalyst for synthesis gas production. *Mol. Catal.* **2022**, *524*, No. 112325.
(38) Barzegari, F.; Rezaei, M.; Kazemeini, M.; Farhadi, F.; Keshavarz, A. R. Effect of rare-earth promoters (Ce, La, Y and Zr) on the catalytic performance of NiO-MgO-SiO2 catalyst in propane dry reforming. *Mol. Catal.* **2022**, *522*, No. 112235.
(39) Barzegari, F.; Kazemeini, M.; Rezaei, M.; Farhadi, F.; Keshavarz, A. R. Syngas production through CO2 reforming of propane over highly active and stable mesoporous NiO-MgO-SiO2 catalysts: Effect of calcination temperature. *Fuel* **2022**, *322*, No. 124211.
(40) Ahmed, T.; Xiu, S.; Wang, L.; Shahbazi, A. Investigation of Ni/Fe/Mg zeolite-supported catalysts in steam reforming of tar using simulated-toluene as model compound. *Fuel* **2018**, *211*, 566−571.
(41) Coenen, K.; Gallucci, F.; Mezari, B.; Hensen, E.; van Sint Annaland, M. An in-situ IR study on the adsorption of CO2 and H2O on hydrotalcites. *J. CO2 Util.* **2018**, *24*, 228−239.
(42) Hahn, M. W.; Steib, M.; Jentys, A.; Lercher, J. A. Tailoring hierarchically structured SiO2 spheres for high pressure CO2 adsorption. *J. Mater. Chem. A* **2014**, *2* (33), 13624−13634.
(43) Jayaprakash, S.; Dewangan, N.; Jangam, A.; Kawi, S. H2S-resistant CeO2-NiO-MgO-Al2O3 LDH-derived catalysts for steam reforming of toluene. *Fuel Process. Technol.* **2021**, *219*, No. 106871, DOI: 10.1016/j.fuproc.2021.106871.
(44) Mihet, M.; Dan, M.; Barbu-Tudoran, L.; Lazar, M. D. CO2 methanation using multimodal Ni/SiO2 catalysts: effect of support modification by MgO, CeO2, and La2O3. *Catalysts* **2021**, *11* (4), 443.
(45) Kasim, S. O.; Al-Fatesh, A. S.; Ibrahim, A. A.; Kumar, R.; Abasaeed, A. E.; Fakeeha, A. H. Impact of Ce-loading on Ni-catalyst supported over La2O3 + ZrO2 in methane reforming with CO2. *Int. J. Hydrogen Energy* **2020**, *45* (58), 33343−33351.
(46) Ibrahim, A. A.; Al-Fatesh, A. S.; Kumar, N. S.; Abasaeed, A. E.; Kasim, S. O.; Fakeeha, A. H. Dry reforming of methane using Ce-modified Ni supported on 8% PO4 + ZrO2 catalysts. *Catalysts* **2020**, *10* (2), 242.
(47) Liu, C.; Cundari, T. R.; Wilson, A. K. CO2 reduction on transition metal (Fe, Co, Ni, and Cu) surfaces: In comparison with homogeneous catalysis. *J. Phys. Chem. C* **2012**, *116* (9), 5681−5688.
(48) Ko, J.; Kim, B.-K.; Han, J. W. Density functional theory study for catalytic activation and dissociation of CO2 on bimetallic alloy surfaces. *J. Phys. Chem. C* **2016**, *120* (6), 3438−3447.

https://doi.org/10.1021/acsomega.4c01338
ACS Omega 2024, 9, 17646−17654